Journal of Sound and Vibration (1999) **228**(1), 11–35
Article No. jsvi.1999.2404, available online at http://www.idealibrary.com on IDEAL®

ANISOTROPY EFFECTS ON THE VIBRATION OF CIRCULAR RINGS MADE FROM CRYSTALLINE SILICON

R. Eley, C. H. J. Fox and S. McWilliam

School of Mechanical, Materials, Manufacturing Engineering & Management, University of Nottingham, University Park, Nottingham NG7 2RD, England

(*Received* 17 *February* 1999, *and in final form* 17 *May* 1999)

Micro-engineered transducers, such as vibratory gyroscopes, accelerometers and pressure transducers made from wafers of crystalline silicon, are becoming increasingly common. These often contain ring-like components, the vibration properties of which are crucial to the operation of the transducer. The stability of the material properties of crystalline silicon is highly beneficial to the performance of these devices. However, the material has significant anisotropy, which must be properly accounted for in the design of the structure. Crystalline silicon has a cubic structure with three principal planes. Two of these, the (111) and (100) planes, are of particular interest since many devices are manufactured from silicon wafers that are nominally cut parallel to these planes. The precise cut of silicon with respect to the principal planes determines the form and degree of anisotropy in the material properties around a structure. This paper focuses on the effects of anisotropy on the natural frequencies and directional properties of the modes of circular rings of rectangular cross-section, made from crystalline silicon. Both in-plane and out-of-plane flexural modes are investigated using Lagrange's equations. The effects of anisotropy are accounted for in the strain energy formulation. General equations are given for directional variations in the elastic moduli. These equations have been simplified and linearized to allow analytical expressions for the natural frequencies to be obtained for a number of special cases. Results are presented for rings made from wafers that are cut nominally in the (100) and (111) principal planes. The effects of small departures in the plane of the wafer cut from these principal planes is investigated. Frequency splitting is predicted between pairs of similar modes which would be degenerate with equal natural frequencies, if the ring were made from an isotropic material. Differences are found between the frequency predictions obtained using general and simplified expressions for the elasitic moduli. These are explained on the basis of a Fourier analysis of the variation in the elastic properties around the ring.

1. INTRODUCTION

There is large and rapidly increasing market for low cost, miniaturized rate gyroscopes and accelerometers. These are required for applications as diverse as automotive safety and navigation, bio-mechanics and aids for the disabled, and virtual reality. Developments in micro-engineering techniques offer significant advantages for the manufacture of small devices in terms of cost and volume of

0022-460X/99/460011 + 25 $30.00/0

production. Several designs of rate gyroscope are available which rely on the inertial properties of a vibrating structure. One successful device is based on a vibrating, micromachined silicon ring structure [1] and others are based on cylinders and hemispherical shells. When designing such instruments, the effects of small variations in component dimensions and material properties must be carefully considered because of their effects on natural frequencies, which must be very accurately controlled. For example, references [2, 3] provide a detailed analysis of the effects of small thickness variations on the in-plane vibration of rings, relevant to the design of vibratory gyroscopes. Increasingly, crystalline silicon is being used as the most suitable material for micro-engineered devices. The stability of its material properties and suitability for forming by micro-machining techniques make the material especially attractive. However, it is well known that crystalline silicon exhibits significant anisotropy, the effects of which must be considered.

Crystalline silicon has three principal planes denoted as (100), (110) and (111) in Miller indices [4]. In practice, mainly due to the capabilities of the etching processes used to form structures from crystalline silicon [5] the (111) and (100) planes are especially important and the vast majority of micro-machined devices are fabricated from silicon wafers which are cut from ingots along the (111) or (100) planes. There is thus a practical need to study the dynamic properties of rings produced from wafers cut in these planes. Furthermore, due to process limitations, it is inevitable that the silicon wafers will not lie exactly in the required planes and the effects of small deviations of the wafer plane from the (111) and (100) need to be considered.

Perfect, circular rings manufactured from isotropic materials have modes of vibration which appear as degenerate pairs at an equal frequency. In practice, small dimensional imperfections and variations in material properties cause small splits between the natural frequencies in a given pair. When a vibrating ring is being used as a rate gyroscope [1, 2] there is a requirement for the natural frequencies of a particular pair of modes to be as closely matched as possible in order to maximize sensitivity. Frequency splits of the order of 0.01% are practically important. The potential effect of material anisotropy to introduce frequency splits is therefore of significant interest. For the reasons given special emphasis will be placed on the elastic properties of silicon in planes which lie close to the (111) and (100) planes. The present paper is structured as follows.

A brief review of the relevant, established anisotropic stress–strain relationships for crystalline silicon is given. These can be manipulated to give general expressions for the elastic moduli on any plane once the direction cosines with respect to the crystal axes are known [6–8]. Reference [9] particularizes the general elastic modulus expressions to predict material property variations in planes which depart by small angles from the principal (111) plane. Using the same approach, the present paper develops expressions for the directional variations of the elastic moduli in the (100) plane and in planes close to it. These expressions are presented in general form and also in a simplified form for small angles of deviation from the principal planes. Once the appropriate material property relationships are established, the natural frequencies, both for in-plane and out-of-plane modes of

vibration, are investigated, via Lagrange's equations using generalized co-ordinates which are based on the eigenvectors for isotropic circular rings. The effects of anisotropy are accounted for in the strain energy. It is convenient to consider the (111) and (100) planes separately.

Finally, numerical examples are given for in-plane and out-of-plane modes with different numbers of nodal diameters. The relationship between the material property variations and number of nodal diameters is investigated. The combinations which lead to frequency splitting are explained using results from a Fourier analysis of the material property variations.

2. ANISOTROPY IN SINGLE-CRYSTAL SILICON

Crystalline silicon has a face-centred cubic diamond structure [4]. In such crystals, the inter-atomic bonding responsible for linear elastic behaviour is intrinsically anisotropic. The resulting, direction dependent, variation of the elastic constants is of specific interest because it affects the natural frequencies of structures, such as rings, made from crystalline silicon. It is useful at this point to summarize the principal results of anisotropic linear elasticity which are relevant to the current work.

The general relationship between the normal (σ_1, σ_2, σ_3), and shear (τ_{12}, τ_{31}, τ_{23}) stresses and the direct (ε_1, ε_2, ε_3) and shear (γ_{12}, γ_{23}, γ_{31}) strains on the faces of the crystal cube (see Figure 1) is well known [7], and can be expressed as

$$\begin{Bmatrix} \varepsilon_1 \\ \varepsilon_2 \\ \varepsilon_3 \\ \gamma_{23} \\ \gamma_{31} \\ \gamma_{12} \end{Bmatrix} = \begin{bmatrix} S_{11} & S_{12} & S_{12} & 0 & 0 & 0 \\ S_{12} & S_{11} & S_{12} & 0 & 0 & 0 \\ S_{12} & S_{12} & S_{11} & 0 & 0 & 0 \\ 0 & 0 & 0 & S_{44} & 0 & 0 \\ 0 & 0 & 0 & 0 & S_{44} & 0 \\ 0 & 0 & 0 & 0 & 0 & S_{44} \end{bmatrix} \begin{Bmatrix} \sigma_1 \\ \sigma_2 \\ \sigma_3 \\ \tau_{23} \\ \tau_{31} \\ \tau_{12} \end{Bmatrix}, \tag{1}$$

where S_{11}, S_{12} and S_{44} are independent elastic compliance constants which, for crystalline silicon, have the following values [8]: $S_{11} = 7{\cdot}6442 \times 10^{-12}\,\mathrm{Pa}^{-1}$, $S_{12} = -2{\cdot}1434 \times 10^{-12}\,\mathrm{Pa}^{-1}$ and $S_{44} = 1{\cdot}2564 \times 10^{-11}\,\mathrm{Pa}^{-1}$.

A cubic material has three principal planes, denoted as (100), (110) and (111) in Miller indices, as illustrated in Figure 2. The cut of silicon wafer with respect to these principal planes determines the extent of anisotropy and the variations in the material properties in devices made from the wafer. Generally, the directional variations of the Young's and shear moduli are given by equations (2) and (3) respectively [9]:

$$\frac{1}{E(\theta)} = S_{11} - 2\left(S_{11} - S_{12} - \frac{S_{44}}{2}\right)F(\theta), \tag{2}$$

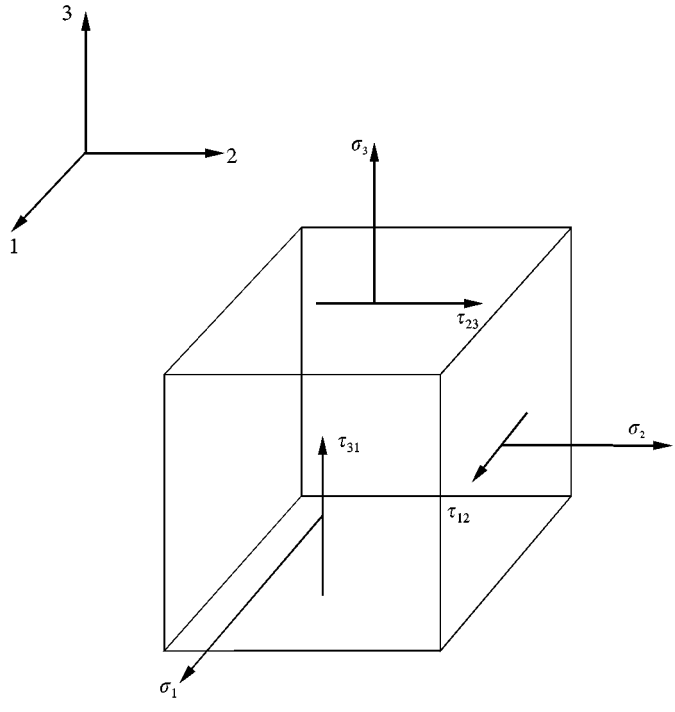

Figure 1. Stress components on a cubic crystal.

$$\frac{1}{G(\theta)} = S_{44} + 4\left(S_{11} - S_{12} - \frac{S_{44}}{2}\right)F(\theta), \tag{3}$$

where

$$F(\theta) = l_s^2 m_s^2 + l_s^2 n_s^2 + m_s^2 n_s^2, \tag{4}$$

and l_s, m_s, and n_s are the direction cosines of a line of applied stress with respect to the material axes X, Y, Z respectively. The argument (θ) simply denotes that the line of applied stress lies at an angle θ from a suitable reference direction in a plane which, for the moment, is arbitrary. Relevant particular cases will be defined later. Expression (4), involving the direction cosines, can be manipulated for different orientations of applied stress, and is a key relationship in the development of the analysis.

3. MATERIAL PROPERTIES CLOSE TO (111) AND (100) PLANES

Devices are commonly manufactured from silicon wafers that are nominally cut in the (111) and (100) planes. It can be shown that the (111) plane has isotropic elastic moduli. Hence, material properties do not vary with direction within this plane, which is unique and ideal for some applications. Unfortunately, manufacturing tolerances on the alignment of cut of silicon wafer relative to the

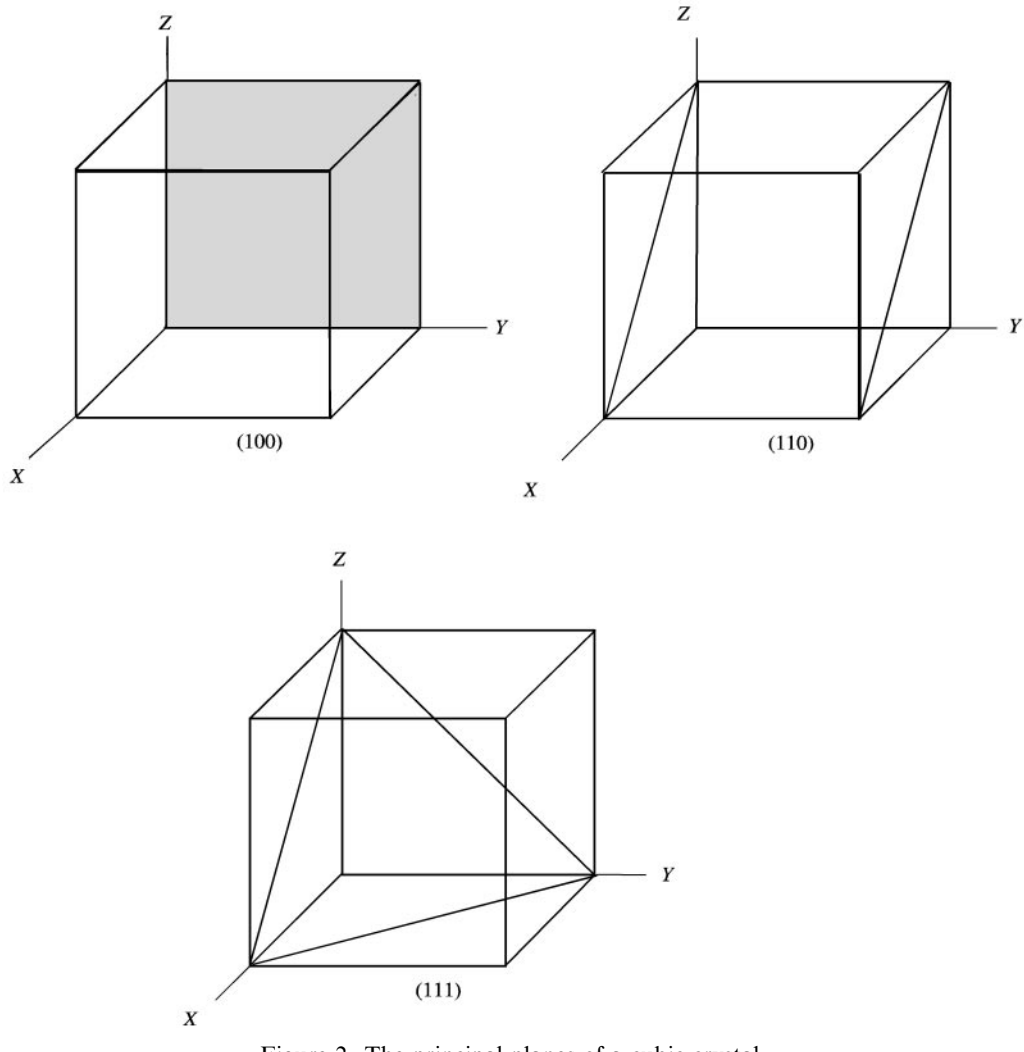

Figure 2. The principal planes of a cubic crystal.

(111) plane lead to variations in the material properties. In the (100) plane, the material properties are anisotropic and vary with direction in the plane. Misalignment of the cut of the wafer relative to the (100) plane leads to additional variations in the moduli.

The general equations, equations (2) and (3), for the material properties can be used to calculate the variations in Young's and shear moduli in any plane, once the direction cosines of the line of applied stress are known. A convenient way to achieve this for our present purposes, is to manipulate expression (4) to find the direction cosines of lines of applied stress in planes which lie at some known angle relative to the principal planes. This is explained in detail for two particular cases in the following section.

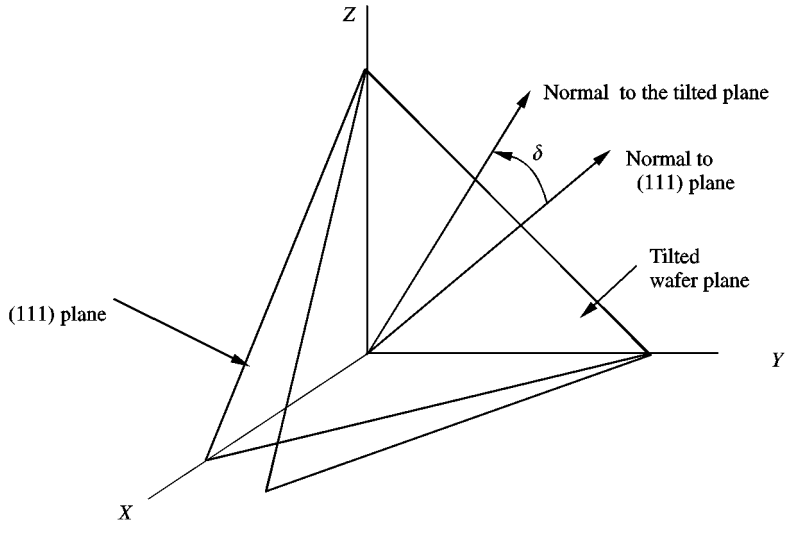

Figure 3. Definition of a plane tilted from the (111) plane.

3.1. ELASTIC CONSTANTS ON PLANES TILTED FROM THE (111) PLANE

The (111) plane is practically important since the material properties are isotropic. Small deviations from this plane need to be considered since they introduce variations in the material properties.

Refer to Figure 3 and consider the (111) plane, the normal to which has equal direction cosines ($1/\sqrt{3}$), relative to the material axes X, Y, Z. By varying one direction cosine, say l_p, and keeping the other two equal, ($m_p = n_p$), a new tilted plane is made, which makes angle δ with the (111) plane. In the tilted plane, the angular variations of the Young's and shear moduli are calculated by considering a line of applied stress which lies in the plane at angle θ relative to a given reference line. The reference line and the line of applied stress have direction cosines (l_r, m_r, n_r) and (l_s, m_s, n_s) respectively. To simplify the analysis, without loss of generality, the reference line is chosen to lie in the y–z plane so that $l_r = 0$ (see Figure 3).

The normal to the tilted plane is perpendicular to both the line of applied stress and to the reference line and has direction cosines (l_p, m_p, n_p) where only l_p is varied.

The direction cosines of the line of applied stress can be found in terms of known quantities as follows. Recall that the angle θ between two intersecting lines is given by

$$l_1 l_2 + m_1 m_2 + n_1 n_2 = \cos\theta, \tag{5}$$

where l_1, m_1, n_1 and l_2, m_2, n_2 are the direction cosines of the lines [10].

It follows for any line with direction cosines (l, m, n) that

$$l^2 + m^2 + n^2 = 1. \tag{6}$$

Equations (5) and (6) can be manipulated using the direction cosines of the reference line, the line of applied stress and the normal to the tilted plane. For the case where

$m_p = n_p$ and $l_r = 0$, it can be shown that

$$m_p^2 = n_p^2 = \tfrac{1}{2}(1 - l_p^2), \tag{7}$$

$$n_r = -m_r = \frac{1}{\sqrt{2}} \tag{8}$$

and

$$l_s = \frac{m_p}{l_p}(\sqrt{2}\cos\theta - 2n_s), \qquad m_s = n_s - \sqrt{2}\cos\theta. \tag{9}$$

Substituting equation (9) into equation (6) for the line of applied stress, it follows that

$$n_s = \frac{\sqrt{2}}{2}\cos\theta + \frac{\sqrt{8}l_p\sin\theta}{4(2m_p^2 + l_p^2)}. \tag{10}$$

Equations (9) and (10) can be substituted into expression (4) to give the following expression for $F(\theta)$, for lines in a plane which lies at angle δ (defined by l_p) from the (111) plane:

$$F_{(\delta,\,111)}(\theta) = \left(1 - \frac{3}{2}l_p^2\right)\sin^2\theta\cos^2\theta + l_p^2\left(1 - \frac{3}{4}l_p^2\right)\sin^4\theta + \frac{\cos^4\theta}{4}. \tag{11}$$

The direction cosines for the (111) plane are all equal ($1/\sqrt{3}$). The angle subtended by the (111) plane with respect to the material axes (X, Y, Z) is $\alpha_0 = \cos^{-1}(1/\sqrt{3}) = 54{\cdot}74^\circ$. The direction cosine with respect to the x-axis for a tilted plane whose normal is at an angle δ to the normal of the (111) plane is given by

$$l_p = \cos(\alpha_0 + \delta). \tag{12}$$

[Note that, due to the symmetry associated with the (111) plane, the effect would be the same if we chose to define δ about any line in the (111) plane. The particular reference direction chosen here is simply convenient for the analysis.]

Equations (11) and (12) can now be used in conjunction with equations (2) and (3) to give the elastic moduli for lines in any plane at angle δ to the (111) plane.

It follows from equations (11) and (12) that, for the (111) plane for which $\delta = 0$,

$$F_{(1\,1\,1)}(\theta) = \tfrac{1}{4}. \tag{13}$$

This shows that F is independent of θ for the (111) plane and, consequently, the elastic properties are the same in all directions within the (111) plane. Using equation (13) in conjunction with equations (2) and (3) gives Young's modulus and shear modulus values for the (111) plane as $1{\cdot}7 \times 10^{11}$ Pa and $6{\cdot}22 \times 10^{10}$ Pa respectively. Other values of δ can be substituted into equations (12) to give l_p for any plane whose normal is at an angle δ to the (111) plane normal. Equations (11), (2) and (3) can then be used to find the appropriate elastic moduli.

For illustration, Figure 4 shows the directional variation in the Young's modulus in the (111) plane and in planes which deviate from the (111) plane for values of δ in

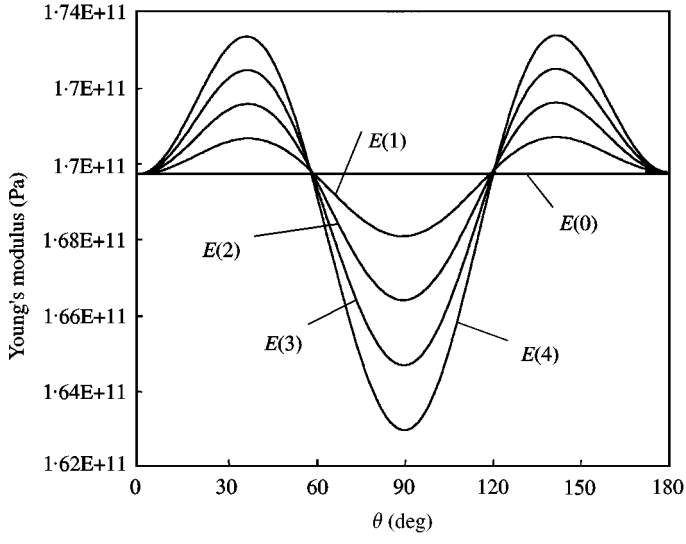

Figure 4. Variations of Young's modulus on planes close to the (111) plane numbers (0), (1), (2), (3), (4) refer to the angle of deviation, δ from the (111) plane.

the range from 1 to 4°. It can be seen that the predominant variations have 2θ and 4θ periodicity. The pattern of variation in the shear modulus is a mirror image about the mean value compared to Figure 4, with the same predominant 2θ and 4θ periodicity. A plane with 4° deviation gives variations of $+2$ and -4% in the Young modulus and $+3$ and -1% in the shear modulus. Other, higher order, variations are present. These are not visually obvious but, as will be shown later, they can be the cause of frequency splitting in some modes.

The reciprocal form of equations (2) and (3) inhibits full interpretation in cases where $F(\theta)$ is not constant. However, for small values of δ, simple forms of equations (2) and (3) can be derived by setting $\sin\delta = \delta$ and $\cos\delta = 1$ in equation (12). Substituting into equation (11) and retaining only linear terms in δ then gives

$$F_{(\delta,111)}(\theta) \approx \tfrac{1}{4} + 0{\cdot}2357\delta(\cos 2\theta - \cos 4\theta). \tag{14}$$

Substitution of equation (14) into equations (2) and (3) allows $E(\theta)$ to be written, after some rearrangement, as

$$E(\theta) \approx \tilde{E}[1 - \tilde{E}e\delta(\cos 2\theta - \cos 4\theta)]^{-1}, \tag{15}$$

where

$$\tilde{E} = 4(2(S_{11} + S_{12}) + S_{44})^{-1} \tag{16}$$

and

$$e = 0{\cdot}4714\left(S_{11} - S_{12} - \frac{S_{44}}{2}\right). \tag{17}$$

$\tilde{E}$ is Young's modulus on the (111) plane with a numerical value of $1{\cdot}7 \times 10^{11}$ Pa and $e = 1{\cdot}65 \times 10^{-12}\,\mathrm{Pa}^{-1}$. Noting that, $\tilde{E}e\delta \ll 1$, the expression in square brackets in equation (15) can be expanded using the binomial expansion. Neglecting terms of second and higher order in δ leads to the following linearized expression:

$$E(\theta) \approx \tilde{E}\{1 + \tilde{E}e\delta(\cos 2\theta - \cos 4\theta)\}. \tag{18}$$

In similar manner, the shear modulus can be expressed as

$$G(\theta) \approx \tilde{G}\{1 - \tilde{G}g\delta(\cos 2\theta - \cos 4\theta)\}, \tag{19}$$

where $\tilde{G}$ $(= 6{\cdot}22 \times 10^{10}\,\mathrm{Pa})$ is the shear modulus on the (111) plane, and $g = 3{\cdot}305 \times 10^{-12}\,\mathrm{Pa}^{-1}$. The practical value of the above approximations will be considered later in the paper when numerical examples are presented.

3.2. ELASTIC CONSTANTS ON PLANES TILTED FROM THE (100) PLANE

The (100) plane of silicon exhibits anisotropy and planes which depart from the (100) plane show additional variations in the elastic moduli. The orientation of a plane which is tilted relative to the (100) plane can be described by means of a rotation about any two of the principal crystal axes or a combination of rotations as shown in Figure 5. Rotation of the (100) plane by γ_1 about the axis OZ, produces plane-1, which is subsequently rotated by γ_2 about the axis OY_1, to give the plane-2. By considering a point on the axis OX_2, which is normal to plane-2 and resolving its co-ordinates into components along the crystal axes $OXYZ$, it can be shown

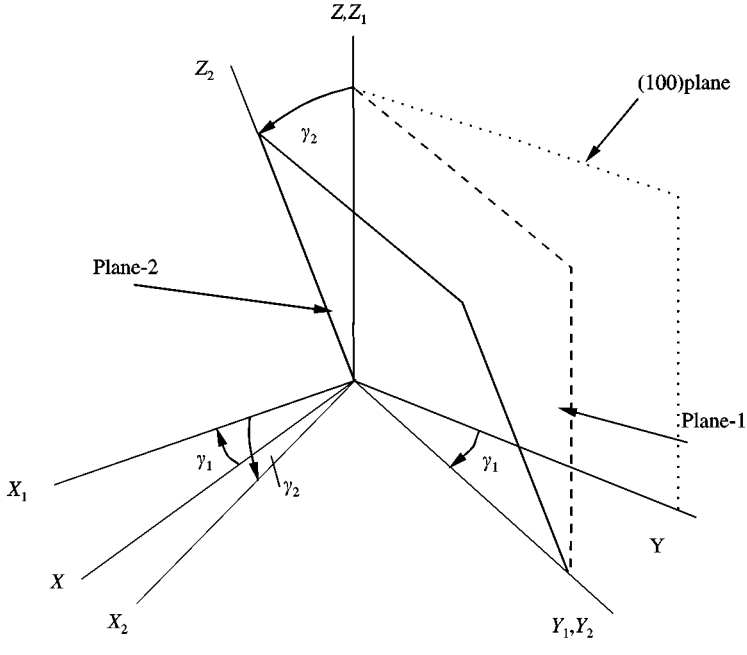

Figure 5. Definition of planes tilted from the (100) plane.

that the direction cosines for the normal to plane-2 relative to the crystal axes are given by

$$l_{np2} = \cos\gamma_1 \cos\gamma_2, \quad m_{np2} = -\sin\gamma_1 \cos\gamma_2, \qquad n_{np2} = -\sin\gamma_2. \tag{20}$$

The reference line from which the direction of loading is defined is conveniently taken to be OY_2 since this line lies in both plane-l and plane-2. It can then be shown that the direction cosines of OY_2 are

$$l_{y2} = \sin\gamma_1, \quad m_{y2} = \cos\gamma_1, \quad n_{y2} = 0. \tag{21}$$

Now consider a line of applied stress (l_s, m_s, n_s) in plane-2 at an angle θ to the reference line. Using equations (5) and (6) for the normal to the plane and the reference line and taking small-angle approximations for γ_1 and γ_2, it can be shown that

$$l_s = \frac{\gamma_1 \cos\theta + \gamma_2 \sin\theta}{\gamma_2^2 + 2\gamma_1^2 + 1}, \quad m_s = \cos\theta - l_s\gamma_1; \quad n_s = \frac{l_s(1-\gamma_1^2) - \gamma_1\cos\theta}{\gamma_2}. \tag{22}$$

Substitution of equations (22), into expression (4) gives the following expression for $F(\theta)$, valid for small deviations from the (100) plane, in which terms in γ_1, γ_2 of third and higher order have been neglected.

$$F_{(\gamma,100)}(\theta) = (1 + 3\gamma_1^2 + 3\gamma_2^2)\sin^2\theta\cos^2\theta + \gamma_1^2\cos^4\theta + \gamma_2^2\sin^4\theta + 2\gamma_1\gamma_2\cos^3\theta\sin\theta. \tag{23}$$

[Note that equation (23) does not contain any terms of order γ. The effect of deviation from the (100) plane only appears in the form of terms of order γ^2. This is in contrast to equation (14) which shows that the effect of small deviations from the (111) plane appear in the corresponding relationship in the form of linear terms of order δ]. Substitution of equation (23) into equations (2) and (3) gives the required expressions for $E(\theta)$ and $G(\theta)$. For the (100) plane for which $\gamma_1 = \gamma_2 = 0$, equation (23) can be written as

$$F_{(100)}(\theta) = \sin^2\theta\cos^2\theta = \tfrac{1}{8}(1 - \cos 4\theta). \tag{24}$$

Hence, there will be a strong 4θ periodicity to the (100) plane moduli, together with higher order harmonics at multiples of 4θ. For silicon, Young's modulus varies by $\sim \pm 13\%$ and the shear modulus by $\sim \pm 12{\cdot}3\%$ about their mean values of $1{\cdot}5 \times 10^{11}$ and $7{\cdot}1 \times 10^{10}$ Pa respectively.

For small deviations from the (100) plane, appropriate values of γ_1 and γ_2 can be substituted into equation (23) to show the variations in moduli. For illustration, Figure 6 shows the directional variation of Young's modulus on the (100) plane and on a plane defined by a 4° rotation (either γ_1 or γ_2) about one of the material principal axes (OY or OZ). The changes due to either γ_1 or γ_2 are small compared to those for deviations from the (111) plane, and are also small compared to the basic variation on the (100) plane. For combined rotations when both γ_1 and γ_2 are non-zero the modulus variations also have 4θ periodicity.

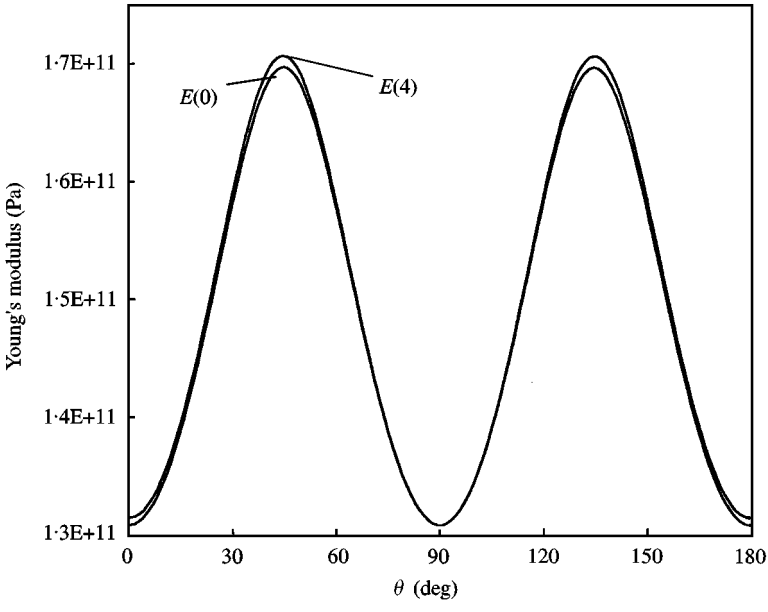

Figure 6. Variations of Young's modulus on planes close to the (100) plane numbers (0), (4) refer to the angle of deviation, γ from the (100) plane.

4. NATURAL FREQUENCIES OF FLEXURAL VIBRATION

The expressions derived in Section 3 can be used in conjunction with an energy method to predict the effects of material anisotropy on the natural frequencies of flexural vibration of circular rings of rectangular cross-section. For a circular ring made from isotropic material, modes with a given harmonic number appear as degenerate pairs. The natural frequencies of the two modes in a given pair are equal and the circumferential position of the modes is arbitrary. Dimensional imperfections are known to introduce splitting between the natural frequencies of mode pairs [11] and fix the mode positions in the ring. It will be demonstrated here that material anisotropy also introduces frequency splitting and fixes the modal positions. The magnitude and pattern of splitting is shown to depend on the plane of the silicon wafer from which the ring is manufactured.

In-plane and out-of-plane vibration are considered separately. The general approach in each case is to consider the behaviour of pairs of modes with a given harmonic number. The displacement of the ring is represented using generalized co-ordinates based on the eigenfunctions of a circular isotropic ring. Lagrange's equation is used to set up equations of motion from which the natural frequencies and the circumferential positions of the corresponding modes can be found for the anisotropic ring.

4.1. IN-PLANE MODES

4.1.1 *Generalized co-ordinates and displacements*

For a pair of in-plane modes of vibration with n nodal diameters, the radial and tangential displacements, w, v, at some angular position θ (see Figure 7), can be

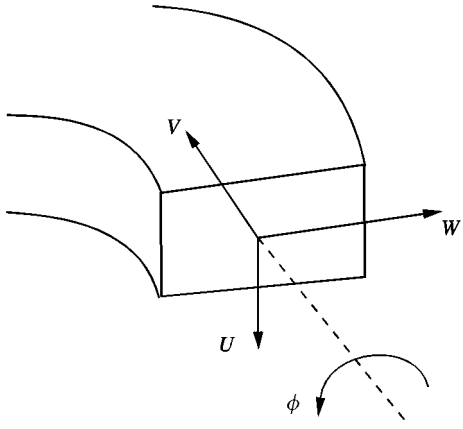

Figure 7. Definition of ring displacement components.

expressed in terms of generalized co-ordinates $Q_{11}(t)$ and $Q_{12}(t)$ as follows [11, 12]:

$$\begin{Bmatrix} w \\ v \end{Bmatrix} = Q_{11}(t) \begin{Bmatrix} n \sin n\theta \\ \cos n\theta \end{Bmatrix} + Q_{12}(t) \begin{Bmatrix} n \cos n\theta \\ -\sin n\theta \end{Bmatrix}. \tag{25}$$

Here, $\theta = 0$ is assumed to coincide with the reference direction for θ used in the expressions for the material properties presented in Section 3.

4.1.2. *In-plane kinetic energy*

For the in-plane modes, the kinetic energy due to bending [13] is given by

$$T_{1P} = \int_0^{2\pi} \frac{1}{2} \rho A a (\dot{v}^2 + \dot{w}^2) \, \mathrm{d}\theta = \frac{\rho A a \pi (n^2 + 1)}{2} (\dot{Q}_{I1}^2 + \dot{Q}_{I2}^2), \tag{26}$$

where ρ, A and a are the density, cross-sectional area and mean radius of the ring respectively.

4.1.3. *In-plane strain energy*

In general terms, assuming the ring to be thin, the strain energy due to in-plane bending, U_{IP}, can expressed as [13]

$$U_{IP} = \frac{I_z}{2a^3} \int_0^{2\pi} E\left(\theta - \frac{\pi}{2}\right) \left[\frac{\partial^2 w}{\partial \theta^2} + w\right]^2 \mathrm{d}\theta, \tag{27}$$

where I_z is the second moment of area of the ring section about the centroidal axis normal to the plane of the ring. The variable Young's modulus, $E(\theta - \pi/2)$, can be expressed in a number of different ways as described in Section 3. The argument $(\theta - \pi/2)$ accounts for the fact that the bending stresses in the ring at position θ are directed at $\pi/2$ to the radius vector at that point. The reciprocal form of equation (2), which defines $E(\theta)$, makes a general analytical evaluation of the integral in equation (27) difficult, if not impossible. In general, therefore, it will be necessary to evaluate equation (27) numerically for particular cases. As an alternative to

numerical integration, the following analytical approach is also presented with the aim of providing data for numerical comparison, and as an aid to insight. In this, the linear approximation of Young's modulus for small deviations from the (111) plane, given by equation (18), will be used so that the strain energy can be expressed as

$$U_{IP} = \frac{\tilde{E}I_z n^2(n^2-1)^2\pi}{2a^3}\left(Q_{I1}^2 + Q_{I2}^2 - \left[\frac{\tilde{E}e\delta}{2}(Q_{I1}^2 - Q_{I2}^2)\right]_{n=2}\right). \tag{28}$$

$n = 1$ corresponds to rigid-body displacement and the resulting zero strain energy is thus expected. The term in square brackets in equation (28) is zero for all n except $n = 2$. This is related to the presence of the cos 4θ term in equation (18).

4.1.4. *In-plane natural frequencies*

The equations of motion for free undamped vibration can now be derived using Lagrange's equation [14] in the form

$$\frac{\mathrm{d}}{\mathrm{d}t}\left(\frac{\partial T}{\partial \dot{Q}_p}\right) - \frac{\partial T}{\partial Q_p} + \frac{\partial U}{\partial Q_p} = 0, \quad p = I1, I2, \tag{29}$$

where T and U are the kinetic and strain energies respectively. Substituting equations (26) and (28) into equation (29) it can be shown that the in-plane equations of motion are given by

$$\begin{aligned} \ddot{Q}_{I1} + \frac{\tilde{E}I_z n^2(n^2-1)^2}{\rho A a^4(n^2+1)}\left(1 - \left[\frac{\tilde{E}e\delta}{2}\right]_{n=2}\right)Q_{I1} = 0, \\ \ddot{Q}_{I2} + \frac{\tilde{E}I_z n^2(n^2-1)^2}{\rho A a^4(n^2+1)}\left(1 + \left[\frac{\tilde{E}e\delta}{2}\right]_{n=2}\right)Q_{I2} = 0. \end{aligned} \tag{30}$$

It follows from equations (30) that the natural frequencies, ω_{I1} and ω_{I2}, of a pair of in-plane modes with a given value of n can be expressed in non-dimensional form as follows:

$$\Omega_{I1}^2 = \frac{\omega_{I1}^2}{f_I^2} = \frac{n^2(n^2-1)^2}{(n^2+1)}\left(1 - \left[\frac{\tilde{E}e\delta}{2}\right]_{n=2}\right), \tag{31}$$

$$\Omega_{I2}^2 = \frac{\omega_{I2}^2}{f_I^2} = \frac{n^2(n^2-1)^2}{(n^2+1)}\left(1 + \left[\frac{\tilde{E}e\delta}{2}\right]_{n=2}\right), \tag{32}$$

where $f_I^2 = \tilde{E}I_z/\rho A a^4$.

The fact that the equations of motion, equations (30), occur as an uncoupled pair indicates that the mode shapes of the orthotropic ring are aligned with the original displacement patterns associated with the relevant generalized co-ordinate. This is a consequence of the choice of datum for θ for the generalized co-ordinates and for the anisotropy description, and of the symmetry of the anisotropy about $\theta = 0$.

For the case where the material properties are isotropic, ($\delta = 0$), equations (31) and (32) lead to the expected conclusion that the natural frequencies will be the same for a pair of modes with the same value of n. It will be noted that they also imply that, using the linear approximation for the material properties when $\delta \neq 0$,

frequency-splitting is only predicted for the case where $n = 2$. This matter will be revisited later.

4.2. OUT-OF-PLANE MODES

The general procedure for dealing with out-of-plane modes is the same as that used for in-plane modes.

4.2.1. *Generalized co-ordinates and displacements*

For out-of-plane modes of vibration, the displacement of the ring section consists of a combination of translation, u, normal to the plane of the ring, and rotation, ϕ, about the centroidal axis, as shown in Figure 7. Introducing out-of-plane generalized co-ordinates, Q_{O1} and Q_{O2}, the displacements for modes with i nodal diameters can be expressed as [12]

$$\begin{Bmatrix} u \\ \phi \end{Bmatrix} = Q_{O1}(t) \begin{Bmatrix} 1 \\ -i^2\xi \end{Bmatrix} \cos i\theta + Q_{O2}(t) \begin{Bmatrix} -1 \\ i^2\xi \end{Bmatrix} \sin i\theta \tag{33}$$

in which

$$\xi = \frac{1}{a}\left[\frac{1+\mu}{1+i^2\mu}\right] \quad \text{where } \mu = \frac{\tilde{G}C}{\tilde{E}I_x} \text{ and } C = \frac{cr_t^3 a_l^3}{r_t^2 + a_l^2}.$$

In the above, a is the mean radius of the ring, r_t and a_l are the radial thickness and axial length of the ring respectively and c is a coefficient with numerical value in the range 0·28–0·33 [12], which depends on the ratio r_t/a_l: I_x is the second moment of area of the ring section for out-of-plane bending. In the present analysis, the assumed displacements associated with the generalized co-ordinates are based on the mode shapes of isotropic rings. It is therefore reasonable to use the (111)-plane values, $\tilde{E}$ and $\tilde{G}$, of the elastic moduli to define the stiffness ratio, μ.

4.2.2. *Out-of-plane kinetic energy*

For out-of-plane motion, the kinetic energy, due to bending and twisting, is given by

$$\begin{aligned} T_{OP} &= \int_0^{2\pi} \frac{1}{2}\rho A a \dot{u}^2 \,\mathrm{d}\theta + \int_0^{2\pi} \frac{1}{2}\rho J a \dot{\phi}^2 \,\mathrm{d}\theta \\ &= \frac{\rho a \pi}{2}\left\{A + \frac{Ji^4}{a^2}\left[\frac{1+\mu}{1+i^2\mu}\right]^2\right\}(\dot{Q}_{O1}^2 + \dot{Q}_{O2}^2), \end{aligned} \tag{34}$$

where J is the polar second moment of area of the ring sections.

4.2.3. *Out-of-plane strain energy*

The strain energy due to bending and twisting [15] can be expressed as

$$U_{OP} = \frac{I_x a}{2}\int_0^{2\pi} E\left(\theta - \frac{\pi}{2}\right) K_1^2 \,\mathrm{d}\theta + \frac{Ca}{2}\int_0^{2\pi} G\left(\theta - \frac{\pi}{2}\right) K_2^2 \,\mathrm{d}\theta \tag{35}$$

where

$$K_1 = \frac{1}{a}\left(\frac{1}{a}\frac{\partial^2 u}{\partial\theta^2} - \phi\right), \qquad K_2 = \frac{1}{a}\left(\frac{\partial\phi}{\partial\theta} + \frac{1}{a}\frac{\partial u}{\partial\theta}\right). \tag{36}$$

In general, equation (35) can be evaluated numerically for any $E(\theta)$ and $G(\theta)$. If, however, the linear approximations for the elastic moduli on planes at a small angle δ from the (111) plane, given by equations (18) and (19), are substituted into equation (35), the out-of-plane strain energy U_{OP} follows as

$$\begin{aligned} U_{OP} = {} & \frac{\tilde{E}I_x\pi i^4(i^2-1)^2\mu^2}{2a^3(1+i^2\mu)^2}\left(Q_{O1}^2 + Q_{O2}^2 + \left[\frac{\tilde{E}e\delta}{2}(Q_{O2}^2 - Q_{O1}^2)\right]_{i=2}\right) \\ & + \frac{\tilde{G}C\pi i^2(i^2-1)^2}{2a^3(1+i^2\mu)^2}\left(Q_{O1}^2 + Q_{O2}^2 + \left[\frac{\tilde{G}g\delta}{2}(Q_{O2}^2 - Q_{O1}^2)\right]_{i=2}\right). \end{aligned} \tag{37}$$

As with the in-plane modes, $i = 1$ indicates rigid-body motion and the corresponding strain energy is zero. Furthermore, the term in square brackets in equation (37) is zero for all i except for $i = 2$.

4.2.4. *Out-of-plane natural frequencies*

Substituting equations (34) and (37) into equation (29) gives the equations of motion for out-of-plane modes as

$$\ddot{Q}_{O1} + \omega_{O1}^2 Q_{O1} = 0, \qquad \ddot{Q}_{O2} + \omega_{O2}^2 Q_{O2} = 0 \tag{38}$$

in which the natural frequencies can be expressed non-dimensionally as

$$\Omega_{O1}^2 = \frac{\omega_{O1}^2}{f_O^2} = \frac{i^2(i^2-1)^2\mu}{(1+i^2\mu)^2 + d^2 i^4(1+\mu)^2}\left\{(1+i^2\mu) + \left[\frac{\delta}{2}(\tilde{G}g + i^2\mu\tilde{E}e)\right]_{i=2}\right\}, \tag{39}$$

$$\Omega_{O2}^2 = \frac{\omega_{O2}^2}{f_O^2} = \frac{i^2(i^2-1)^2\mu}{(1+i^2\mu)^2 + d^2 i^4(1+\mu)^2}\left\{(1+i^2\mu) - \left[\frac{\delta}{2}(\tilde{G}g + i^2\mu\tilde{E}e)\right]_{i=2}\right\}, \tag{40}$$

where $f_O^2 = \tilde{E}I_x/\rho A a^4$ and $d^2 = J/Aa^2$.

As in the case of the in-plane modes, the equations of motion, equations (38), are uncoupled. Again, this is due to the choice of datum for θ and the symmetry of the anisotropy about $\theta = 0$.

5. NUMERICAL EXAMPLES

As indicated in section 4, when calculating the natural frequencies the strain energy can be evaluated either numerically or analytically, depending on the complexity of the expressions for the variation in the elastic moduli. Results will be presented for natural frequencies calculated numerically using the full expressions for the elastic moduli (equations (2), (3), (11) and (12)) on planes at small angular deviations from the (111) plane. They are compared with the analytical expressions (equations (31), (32), (39) and (40)) obtained using the linearized expressions.

Frequency variations obtained numerically using elastic moduli for the (100) plane and increasing deviations from this plane are also shown. The numerical values given apply for a silicon ring for which $d^2 = 8{\cdot}83 \times 10^{-4}$ in equations (39) and (40).

5.1. FREQUENCY SPLITS IN RINGS CLOSE TO THE (111) PLANE

5.1.1. *Using exact expressions for the elastic moduli*

The natural frequencies have been calculated using the exact expressions for the elastic moduli given by equations (2) and (3) and the appropriate expression for $F(\theta)$, equation (11). These have been substituted into the strain energy expressions, equations (27) and (35) respectively, for in-plane and out-of-plane modes. Numerical results are shown for small deviations in the range 0–4°, from the (111) plane and for modes with two, three and four nodal diameters. The corresponding frequency predictions, obtained using the simplified expressions for the elastic moduli, equations (18), (19), (31) and (32), are given in section 5.1.2.

5.1.1.1. *Fourier analysis of elastic moduli.* To help explain the differences between the two sets of natural frequency predictions, it is useful to consider the harmonic content of the elastic modulus variations with respect to θ, which defines the direction of the line of applied stress. It is clear from equations (18) and (19) that the simplified expressions only contain 2θ and 4θ components. However, a Fourier analysis of the general expressions for $E(\theta)$ and $G(\theta)$ shows that other harmonic components are present, although at much reduced magnitude compared to the 2θ and 4θ components. The form of equations (2), (3), (11) and (12) precludes a simple analytical determination of the Fourier coefficients when $\delta \neq 0$ and they have been calculated numerically so that $E(\theta)$ can be expressed in the form

$$E(\theta) = E_O + \sum_{m=1}^{M} [E_{mC} \cos m\theta + E_{mS} \sin m\theta].$$

The shear modulus $G(\theta)$ can be treated in the same way.

Table 1 shows the magnitude of the Fourier coefficients of the exact form of $E(\theta)$ on planes close to the (111) plane and, for future reference, also shows the Fourier coefficients of the linearized version of $E(\theta)$ as given by equation (18). It can be seen that, on the (111) plane (i.e., for $\delta = 0$), only the constant term is non-zero. For non-zero values of δ, the Fourier analysis shows a constant component together with even-order harmonic, cosine components. The sine components are all zero, due to the choice of reference direction for θ. For the range of values of δ considered, the 2θ and 4θ cosine components are generally two orders of magnitude smaller than the constant value. The magnitude of each harmonic increases as δ increases. Higher order harmonics are also present, but at a much reduced magnitude. The fact that the odd harmonic components are zero is compatible with the symmetry in the distribution as seen in Figure 4. The absence of the odd-valued harmonics and the sine components allows the expression for the Young's modulus

TABLE 1

Fourier components of exact and linearized $E(\theta)$ close to the (111) plane

δ (deg)	E_0 (Pa)	E_{2C} (Pa)	E_{4C} (Pa)	E_{6C} (Pa)	E_{8C} (Pa)
		Using full expression			
0	$1{\cdot}6974 \times 10^{11}$	0·00	0·00	0·00	0·00
1	$1{\cdot}6973 \times 10^{11}$	$0{\cdot}845 \times 10^{9}$	$-0{\cdot}832 \times 10^{9}$	$-0{\cdot}416 \times 10^{7}$	$0{\cdot}204 \times 10^{7}$
2	$1{\cdot}6970 \times 10^{11}$	$1{\cdot}706 \times 10^{9}$	$-1{\cdot}654 \times 10^{9}$	$-1{\cdot}672 \times 10^{7}$	$0{\cdot}802 \times 10^{7}$
3	$1{\cdot}6964 \times 10^{11}$	$2{\cdot}582 \times 10^{9}$	$-2{\cdot}467 \times 10^{9}$	$-3{\cdot}784 \times 10^{7}$	$1{\cdot}780 \times 10^{7}$
4	$1{\cdot}6957 \times 10^{11}$	$3{\cdot}470 \times 10^{9}$	$-3{\cdot}270 \times 10^{9}$	$-6{\cdot}760 \times 10^{7}$	$3{\cdot}117 \times 10^{7}$
		Using linear expression			
0	$1{\cdot}700 \times 10^{11}$	0·00	0·00		
1	$1{\cdot}700 \times 10^{11}$	$0{\cdot}832 \times 10^{9}$	$-0{\cdot}832 \times 10^{9}$		
2	$1{\cdot}700 \times 10^{11}$	$1{\cdot}665 \times 10^{9}$	$-1{\cdot}665 \times 10^{9}$		
3	$1{\cdot}700 \times 10^{11}$	$2{\cdot}497 \times 10^{9}$	$-2{\cdot}497 \times 10^{9}$		
4	$1{\cdot}700 \times 10^{11}$	$3{\cdot}329 \times 10^{9}$	$-3{\cdot}329 \times 10^{9}$		

to be written in the form

$$E(\theta) = E_o + \sum_{m=2}^{4,6,8,10} E_{mC} \cos m\theta. \tag{41}$$

To see how the spatial harmonic content of the elastic moduli, shown above, influences the pattern of frequency splitting between modes, note that, using equation (41), the integral for the in-plane strain energy, equation (27), can be written in the form

$$U = \frac{I_z}{2a^3} \int_0^{2\pi} \left(E_o + \sum_{m=2}^{4,6,8,10} [E_{mC} \cos m\theta] \right) (W_1 \sin n\theta + W_2 \cos n\theta)^2 \, \mathrm{d}\theta, \tag{42}$$

where W_1 and W_2 are the amplitudes of the displacement components. When integral (42) is evaluated, the constant part of the elastic modulus, E_o, gives rise to non-zero contributions to the strain energy which depend only on W_1^2 and W_2^2 but not on $W_1 W_2$. The terms involving E_{mC} give rise to integrals of the form

$$I = E_{mC} \int_0^{2\pi} \cos m\theta [W_{1,2}^2 \cos 2n\theta + W_1 W_2 \sin 2n\theta] \, \mathrm{d}\theta. \tag{43}$$

The outcome of the integral, equation (43), is zero for $m \neq 2n$ but non-zero when $m = 2n$, in which case the sign of W will be different depending on whether the integral involves W_1 or W_2. This implies that the natural frequencies of pairs of modes with n nodal diameters will be split when $m = 2n$. Thus, the Fourier analysis indicates that for non-zero values of δ, the exact expressions for the moduli will lead to predicted frequency splits in modes for which $n = 2, 3, 4, 5, \ldots$. On the (111) plane absence of any harmonics means that the natural frequencies of a pair of modes will be equal for a given value of n.

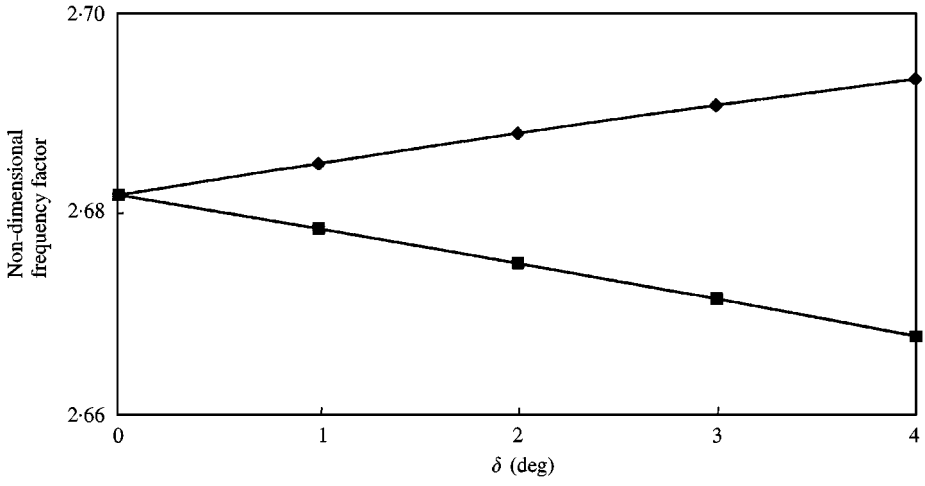

Figure 8. Effect of deviation from the (111) plane on frequency factor for in-plane modes with $n = 2$ (exact expression for $E(\theta)$).

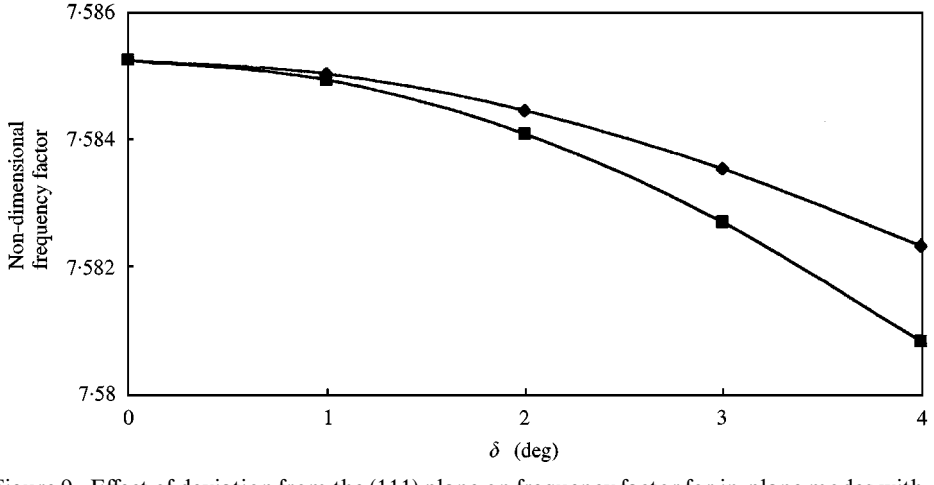

Figure 9. Effect of deviation from the (111) plane on frequency factor for in-plane modes with $n = 3$ (exact expression for $E(\theta)$).

5.1.1.2. *In-plane modes.* Figure 8 shows the variation in non-dimensional natural frequencies, Ω_{11}, Ω_{12}, obtained numerically using the full expressions for the elastic moduli, for in-plane modes with $n = 2$. As expected the frequency values are equal on the (111) plane where the material properties are isotropic. As the angle of deviation increases, one frequency increases whilst the other decreases. Both values show a sensibly linear variation with angle of deviation from the (111) plane for the range of values of δ considered and the split is symmetrical about the (111) value. Figures 9 and 10 show the variation of the natural frequencies of the modes for which $n = 3$ and 4. The pattern of behaviour is somewhat different for these modes. Both frequencies in a given pair decrease slightly and frequency splitting is

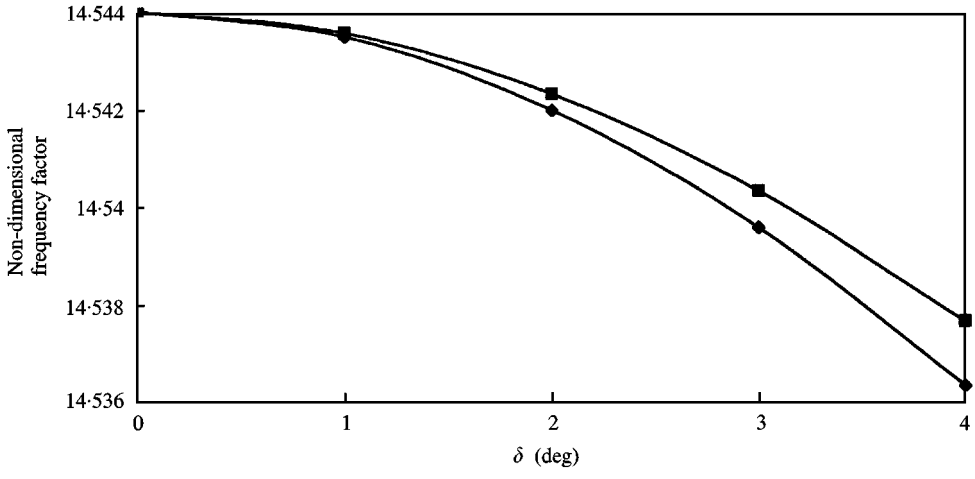

Figure 10. Effect of deviation from the (111) plane on frequency factor for in-plane modes with $n = 4$ (exact expression for $E(\theta)$).

observed, albeit at a much reduced level compared to the $n = 2$ modes. This is compatible with the fact the 6θ and 8θ coefficients of $E(\theta)$ are two orders of magnitude smaller than the 4θ component. The slight reduction in both frequencies for $n = 3$ and 4 is associated with the slight reduction in $E(\theta)$ as δ increases. Therefore, it is expected that when $n = 2$ the frequencies will be affected greatest and for higher values of nodal diameter the effects of anisotropy are reduced. A deviation of 4° produces frequency splits of 0·97, 0·02 and 0·01% of the (111) values, respectively, in the natural frequencies of modes for which $n = 2$, 3 and 4.

5.1.1.3. *Out-of-plane modes.* Table 2 shows the predicted natural frequencies of out-of-plane modes for $i = 2, 3, 4$. Each pair of out-of-plane modes with the same value of i has equal natural frequencies on the (111) plane, as expected. The variation of the natural frequencies with deviation from the (111) plane is very similar to those presented for the in-plane modes as shown in Figures 8–10. When $i = 2$, the frequencies vary sensibly linearly, one increasing and one decreasing. The frequencies of modes for which $i = 3$ and 4 both decrease as the angle of deviation increases from the (111) plane. The frequency splits at an angle of deviation of 4° are 0·92, 0·02 and 0·01% of the value on the (111) plane for modes for which $i = 2$, 3 and 4 respectively.

The explanation of the pattern of frequency splitting in relation to the Fourier coefficients of $E(\theta)$ and $G(\theta)$ is the same as that given for in-plane modes.

5.1.2. *Using linearized expressions for the elastic moduli*

The linearized expressions for the material properties, equations (18) and (19), are derived from a binomial expansion of equations (2) and (3) with $F(\theta)$, given by equation (14), where only the linear term in δ is retained. It is clear that equations (18) and (19) only contain 2θ and 4θ harmonic variations. Table 1 shows the 2θ and 4θ harmonic components for the linearized expression. It can be seen that the

TABLE 2

Non-dimensional natural frequency factors for out-of-plane modes for planes close to the (111) *plane*

	$i = 2$		$i = 3$		$i = 4$	
δ (deg)	Ω_{O1}	Ω_{O2}	Ω_{O1}	Ω_{O2}	Ω_{O1}	Ω_{O2}
0	2·7002	2·7002	7·6043	7·6043	14·5545	14·5545
1	2·6971	2·7033	7·6040	7·6041	14·5541	14·5540
2	2·6938	2·7063	7·6033	7·6037	14·5530	14·5527
3	2·6905	2·7091	7·6022	7·6030	14·5512	14·5505
4	2·6871	2·7119	7·6007	7·6020	14·5489	14·5477

magnitude of these components differ very little to those obtained from the exact expression, the maximum difference being $\sim 4{\cdot}1\%$ in the 2θ component and $1{\cdot}8\%$ in the 4θ component. Therefore, it is expected that using the linearized expression for $E(\theta)$ in the strain energy integral will lead to predicted splits in the modes with two nodal diameters that are of the same order as those obtained using the exact expression for $E(\theta)$.

If terms of order δ^2 are retained in the binomial expansion, it can easily be shown that the resulting approximate expressions for $E(\theta)$ and $G(\theta)$ would contain 2θ, 4θ, 6θ and 8θ components as seen for the full expressions. The magnitudes of the 2θ and 4θ components differ by only a small amount from the components in the full expression. However, the coefficients of the 6θ and 8θ harmonics are found to be in error by about 50%. These differences would lead to discrepancies in the predicted natural frequencies for modes with three and four nodal diameters. Hence, the linearized version of the binomially expanded expression for the elastic moduli leads to good predictions of natural frequencies for modes with two nodal diameters, but the exact form of $E(\theta)$ and $G(\theta)$ should be used for all other modes.

5.1.2.1. *In-plane modes.* Using the linearized expressions for the elastic moduli, it follows from equations (31) and (32) that the non-dimensional natural frequencies for $n = 2$ modes are given by

$$\Omega_{I1,I2} = \sqrt{\frac{36}{5}\left(1 \pm \frac{\tilde{E}e\delta}{2}\right)}. \tag{44}$$

The frequencies are equal on the (111) plane and as the angle of misalignment increases, one frequency increases and one decreases. If the numerical results from equation (44) were plotted in Figure 8, the points would be visually coincident with the existing points generated using the full expressions for the elastic moduli. At an angle of deviation of 4°, equation (44) gives frequency predictions which are generally within 0·07% of the "exact" predictions and the frequency split is 0·97% of the (111) plane frequency which, to two percentage decimal places, is the same as the prediction obtained using the full expressions.

5.1.2.2. *Out-of-plane modes.* Similarly, for the out-of-plane modes, it follows from equations (39) and (40) that the non-dimensional natural frequencies for $i = 2$ modes are given by

$$\Omega_{O1,O2} = \sqrt{\frac{36\mu}{(1 + 4\mu + 16d^2(1 + \mu)^2)}\left[1 + 4\mu \pm \frac{\delta}{2}(\tilde{G}g + 4\mu\tilde{E}e)\right]}. \tag{45}$$

According to equation (45), the natural frequencies for $i = 2$ vary in a similar manner to that shown by the in-plane $n = 2$ modes. At an angle of deviation of 4°, the frequencies are split by 0·92% which is identical to the predicted split when the full expressions are used. Thus, for modes with two nodal diameters, equations (44) and (45) provide simple and accurate expressions for calculating the natural frequencies of rings which lie close to the (111) plane.

5.2. FREQUENCY SPLITS IN RINGS CLOSE TO THE (100) PLANE

The analysis presented for planes tilted from the (100) plane allows deviations about one crystal axis (γ_1 or γ_2 individually) or a combined rotation (γ_1 and γ_2 simultaneously) to be examined. The variations in elastic moduli are similar if either γ_1 or γ_2 is equal to zero, allowing rotation about one axis only. Equations (2), (3) and (23) which define the elastic moduli on planes at small angular deviations from the (100) plane are substituted into the strain energy expression to show the effects on the natural frequencies.

Table 3 shows the results from a Fourier analysis on the material properties for the (100) plane using equations (23) and (2). On the (100) plane, there is a large constant term together with 4θ, 8θ, 12θ, etc., harmonics of relatively smaller magnitude. This would be expected to give rise to frequency splits only in modes with even numbers of nodal diameters. On planes tilted about one principal axis from the (100) plane, the Fourier analysis shows additional 2θ, 6θ, 10θ, … , components, but these are much smaller ($\times 10^{-2}$–10^{-3}) in magnitude compared to the 4θ and 8θ components. These would give rise to split frequencies for flexural modes with odd numbers of nodal diameters, but the splits will be much smaller due to the magnitude of the corresponding Fourier coefficients of the elastic moduli.

TABLE 3

Fourier components of $E(\theta)$ on planes close to the (100) *plane*

γ_2 (deg) ($\gamma_1 = 0$)	E_0 (Pa)	E_{2C} (Pa)	E_{4C} (Pa)	E_{6C} (Pa)	E_{8C} (Pa)
		Using full expression			
0	$1{\cdot}4901 \times 10^{11}$	0·00	$-1{\cdot}938 \times 10^{10}$	0·00	$1{\cdot}260 \times 10^{9}$
1	$1{\cdot}4905 \times 10^{11}$	$-0{\cdot}208 \times 10^{8}$	$-1{\cdot}940 \times 10^{10}$	$0{\cdot}279 \times 10^{7}$	$1{\cdot}263 \times 10^{9}$
2	$1{\cdot}4916 \times 10^{11}$	$-0{\cdot}833 \times 10^{8}$	$-1{\cdot}946 \times 10^{10}$	$1{\cdot}124 \times 10^{7}$	$1{\cdot}270 \times 10^{9}$
3	$1{\cdot}4935 \times 10^{11}$	$-1{\cdot}880 \times 10^{8}$	$-1{\cdot}957 \times 10^{10}$	$2{\cdot}545 \times 10^{7}$	$1{\cdot}282 \times 10^{9}$
4	$1{\cdot}4961 \times 10^{11}$	$-3{\cdot}350 \times 10^{8}$	$-1{\cdot}972 \times 10^{10}$	$4{\cdot}564 \times 10^{7}$	$1{\cdot}300 \times 10^{9}$

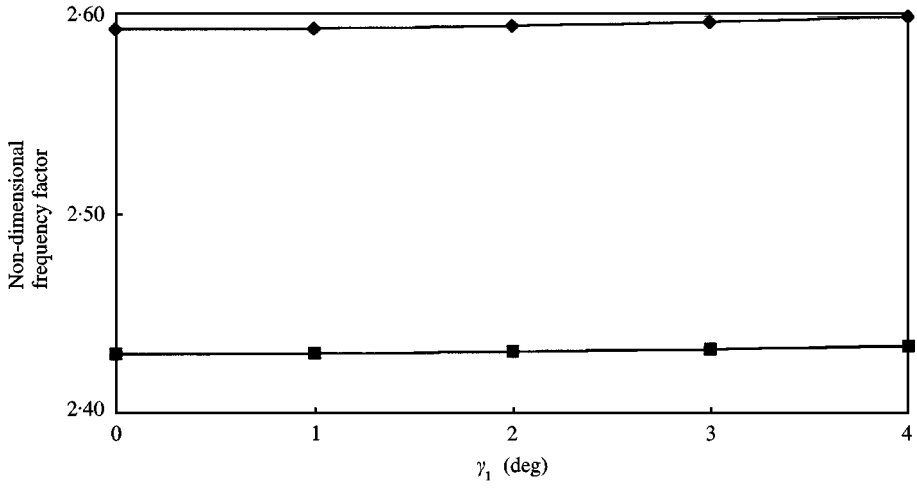

Figure 11. Effect of deviation from the (100) plane on frequency factor for in-plane modes with $n = 2$.

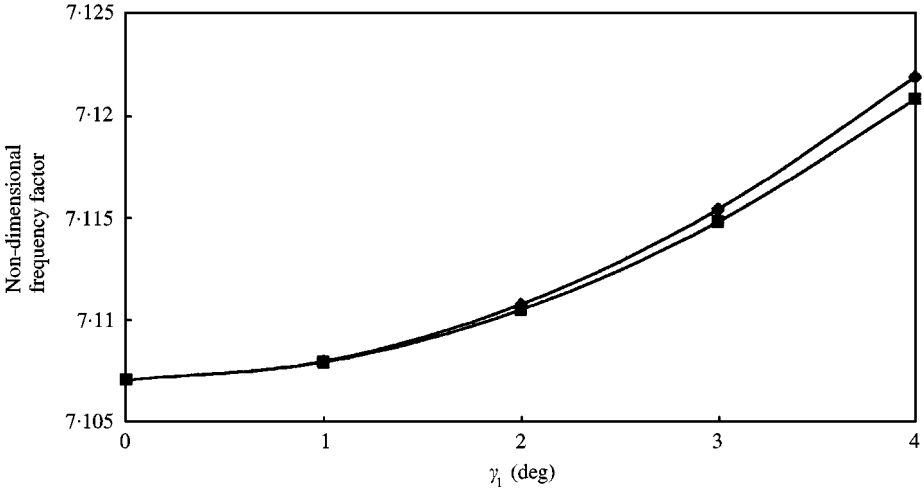

Figure 12. Effect of deviation from the (100) plane on frequency factor for in-plane modes with $n = 3$.

5.2.1. *Deviations about one axis*

5.2.1.1. *In-plane modes.* Figure 11 shows the frequency variations for $n = 2$ modes, which are split on the (100) plane by 6·51%. The upper and lower frequencies increase by 0·24 and 0·15% respectively as the angle of deviation about the principal axis is increased to 4°. The slight increase in both frequencies ($\sim$ 0·2%) is consistent with the small increase ($\sim$ 0·4%) in the Young modulus value. At this maximum rotation, the frequency split is 6·6% of the mean value. For $n = 3$, the natural frequencies are not split on the (100) plane. As the angle of deviation from the (100) plane is increased, both frequencies increase (by $\sim$ 0·2%) and separate to give a split of 0·02% at an angle of 4° as shown in Figure 12. For $n = 4$, Figure 13 shows that the natural frequencies are split by 0·42% on the (100) plane and both

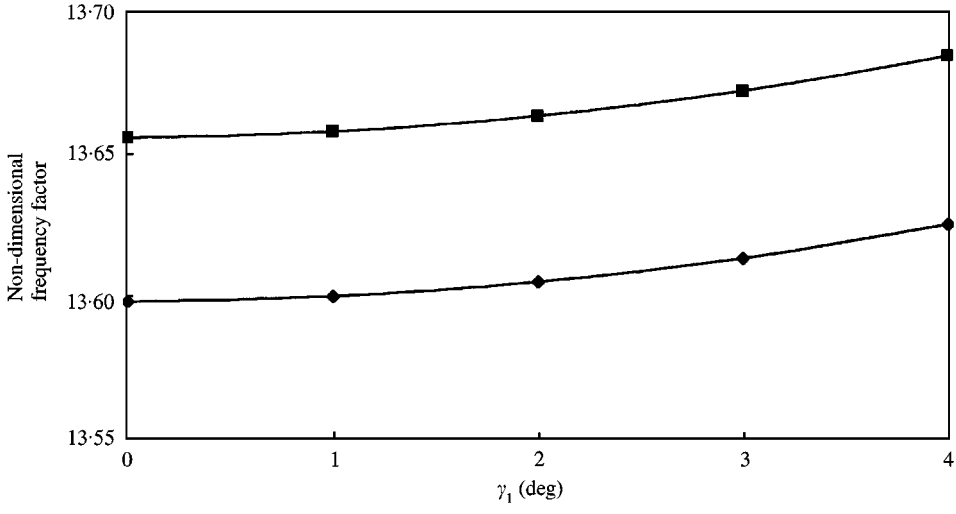

Figure 13. Effect of deviation from the (100) plane on frequency factor for in-plane modes with $n = 4$.

TABLE 4

Non-dimensional natural frequency factors for out-of-plane modes for planes close to the (100) *plane*

	$i = 2$		$i = 3$		$i = 4$	
γ_2 (deg)	Ω_{O1}	Ω_{O2}	Ω_{O1}	Ω_{O2}	Ω_{O1}	Ω_{O2}
0	2·5127	2·6796	7·2198	7·2198	13·7689	13·7185
1	2·5128	2·6798	7·2205	7·2205	13·7705	13·7199
2	2·5132	2·6806	7·2227	7·2225	13·7752	13·7243
3	2·5138	2·6819	7·2264	7·2259	13·7830	13·7316
4	2·5146	2·6837	7·2316	7·2308	13·7939	13·7418

frequencies increase with angle of deviation by $\sim 0{\cdot}2\%$ to give a split of 0·43% at an angle of deviation of 4°. The percentage splits reflect the magnitude of the relevant harmonic components.

5.2.1.2. *Out-of-plane modes.* Table 4 shows the variation in the natural frequencies of the out-of-plane modes. The trend of variation is the same as those shown by the in-plane mode frequencies. On the (100) plane, the natural frequencies for $i = 2$ are split by 6·42%. Both the upper and lower frequencies increase with angle of deviation by 0·15 and 0·07% respectively. This gives a split of 6·5% when the angle rotated is 4°. The $i = 3$ natural frequencies are equal on the (100) plane but separate a little with increasing angle of deviation. The split is 0·01% of the mean value when the angle is 4°. The frequencies for $i = 4$ are split by 0·37% on the (100) plane and this increases to 0·38% at an angle of deviation of 4°. The percentage splits in the

TABLE 5

Non-dimensional natural frequency factors for in-plane modes for planes close to the (100) *plane*

		$n = 2$		$n = 3$		$n = 4$	
γ_1 (deg)	γ_2 (deg)	Ω_{I1}	Ω_{I2}	Ω_{I1}	Ω_{I2}	Ω_{I1}	Ω_{I2}
1	0	2·5929	2·4294	7·1064	7·1064	13·597	13·654
0·866	0·5	2·5929	2·4294	7·1064	7·1064	13·597	13·654
0·707	0·707	2·5929	2·4294	7·1064	7·1064	13·597	13·654
0·5	0·866	2·5929	2·4294	7·1064	7·1064	13·597	13·654
0	1	2·5929	2·4294	7·1064	7·1064	13·597	13·654

frequencies reflects the magnitude of the relevant harmonic components of the elastic moduli.

5.2.2. *Combined rotations*

Combinations of γ_1 and γ_2 which give resultant misalignment of 1, 2, 3 and 4° have also been investigated. For a given *resultant* misalignment angle, there are no practically significant variations in the frequency values for different combinations of γ_1 and γ_2. This is illustrated in Table 5 for a resultant misalignment angle of 1°. To five significant figures, the values are the same as those obtained when a 1° rotation is applied about a single principal axis. The reason for this is illustrated by examining the reciprocal of equation (23) with varying values for γ_1 and γ_2. The amplitudes of the variations are several orders of magnitude smaller than the moduli values and hence are negligible.

6. CONCLUSION

This paper presents an analysis of the effects of anisotropy on the natural frequencies of vibrating rings made from crystalline silicon, with particular emphasis on rings whose planes lie close to the (111) and (100) planes. Expressions are presented for the variations in material properties on these planes due to anisotropy. The periodic directional variations in the material properties due to anisotropy are shown to affect the natural frequencies of pairs of modes of the ring in a way which depends on the number of nodal diameters of the modes in question.

For rings in the (111) plane, the modes occur in pairs of equal frequency since the material properties are isotropic. Misalignment of the plane of the ring from this plane introduces splits in the frequency pairs. The exact expressions for the elastic moduli on planes which deviate by a small angle from the (111) plane contain 2θ, 4θ, 6θ, 8θ and higher order even harmonic components. It is shown that these components will affect the frequencies of flexural modes with 2, 3, 4, … , etc., nodal diameters respectively. The magnitude of the frequency splits depend on the magnitude of the relevant harmonic.

On the (100) plane the material properties are shown to contain 4θ, 8θ, $12\theta \ldots$ harmonics. Hence, rings in the (100) plane have frequencies that are split for modes with 2, 4, 6, … , nodal diameters, but not in modes with 3, 5, 7 … nodal diameters. Misalignment from the (100) plane introduces additional harmonic components in the material properties which will split the frequencies for modes with 3, 5, 7 … nodal diameters, but the splitting in these modes is smaller than in modes with an even number of nodal diameters.

For the cases considered, the effects of anisotropy are most significant for modes with two nodal diameters. Analytical expressions have been developed which can be used to provide simple, accurate estimates of these modes for rings which lie close to the (111) plane.

ACKNOWLEDGMENT

The authors gratefully acknowledge the support for this work provided by British Aerospace Systems and Equipment Ltd and EPSRC through the Industrial CASE scheme.

REFERENCES

1. I. Hopkins 1997 *Proceedings DGON Symposium on Gyro Technology*, *Stuttgart*. Performance and design of a silicon micro-machined gyro.
2. R. S. Hwang, C. H. J. Fox and S. McWilliam 1999 *Journal of Sound and Vibration*. The in-plane vibration of thin rings with in-plane profile variations, Part I: general background and theoretical formulation.
3. C. H. J. Fox, R. S. Hwang and S. McWilliam 1999 *Journal of Sound and Vibration*. The in-plane vibration of thin rings with in-plane profile variations, Part II: application to nominally circular rings.
4. C. Kittel 1996 *Introduction to Solid State Physics*. New York: Wiley, seventh edition.
5. L. Ristic (editor) 1994 *Sensor Technology and Devices*. Artech House.
6. R. M. Jones 1998 *Mechanics of Composite Materials*. London: Taylor and Francis, second edition.
7. T. H. Courtney 1990 *Mechanical Behaviour of Materials*. New York: McGraw-Hill.
8. W. R. Runyan 1965 *Silicon Semiconductor Technology*. New York: McGraw-Hill.
9. *Private Communication* (British Aerospace).
10. J. H. Heading 1970 *Mathematical Methods in Science and Engineering*. London: Edward Arnold.
11. C. H. J. Fox 1990 *Journal of Sound and Vibration* **142**, 227–243. A simple theory for the analysis and correction of frequency splitting in slightly imperfect rings.
12. R. D. Blevins 1995 *Formulas for Natural Frequencies and Mode Shapes*. Krieger.
13. J. Kirkhope 1977 *Journal of Sound and Vibration* **50**, 219–247. In-plane vibrations of thick circular rings.
14. G. B. Warburton 1976 *The Dynamical Behaviour of Structures*. Oxford: Pergamon.
15. J. Kirkhope 1976 *ASCE Journal of the Engineering Mechanics Division* **102**, 239–247. Out-of-plane vibration of thick circular rings.